Supporting information: methods:

Land cover classification

This study employed a land cover classification developed and validated in a previous study in our study area (Gutiérrez-Vélez and DeFries 2013). The original classification spanned 10 years (2000-2010). It differentiates between high-biomass forest, low-biomass forest, and other land cover types, including oil palm, deforested, fallow, pasture, bare soil, and water, with overall accuracy of 93%. For a more detailed accuracy assessment see Gutierrez-Velez and DeFries (2013). We applied the same procedure and classification tree to additional images to complete a 30 year time series with 30x30 m pixel resolution. Specifically, we identified Landsat TM/ETM+ scenes from 1984-1999, and 2011-2013 (Table 1). All scenes were acquired as surface reflectance with atmospheric corrections from the Landsat CDR archive (USGS 2017) via USGS Earth Explorer (http://earthexplorer.usgs.gov). Scenes were radiometrically normalized to a reference image from the year 2000 using the iMAD algorithm (Canty and Nielsen 2008) and clouds and cloud shadows were masked using the Fmask band included in the surface reflectance product (Zhu and Woodcock 2012, Zhu et al. 2015, USGS 2017). We calculated the following band transformations for each image, for use in the classification procedure: 1) tasseled cap band transformations (brightness, greenness, third), 2) bare, vegetation, and shade fractions from spectral mixture analysis, and 3) NDVI. Finally, we applied the previously developed random forest classifier to the transformed bands and masked oil palm plantations with a previously developed map of oil palm in the study area (Gutierrez-Velez and DeFries 2013). To improve accuracy and predict land cover in data gaps or areas covered by clouds when possible, we applied a temporal filter to disallowed trajectories (cite). Remote sensing analyses were conducted in ENVI 4.8 (Exelis Visual Information Solutions).

Field data collection and calculation of forest biomass

To establish the relationship between forest age and biomass accumulation, we used data from 30 field plots. In each plot, we measured all stems > 5 cm diameter at breast heigh (dbh). To determine plot level biomass, we used the following allometric equation developed for secondary forest species in the central Amazon (Nelson et al. 1999):

$$\ln(\text{biomass}) = -1.9968 + 2.4128 * \ln(\text{DBH})$$

We scaled plot-level values to units of Mg/ha, and divided values by two so that estimates were in terms of kg C instead of kg biomass, under the assumption that C makes up 50% of biomass (Brown and Lugo, 1982). We found a highly significant relationship between biomass and forest age ($R^2 = 0.517$, $p > 0.001$, Figure S1).

References

Brown S and Lugo A E 1982 The Storage and Production of Organic Matter in Tropical Forests and Their Role in the Global Carbon Cycle Biotropica 14 161 Online: http://www.jstor.org/stable/2388024?origin=crossref

Canty M J and Nielsen A A 2008 Automatic radiometric normalization of multitemporal satellite imagery with the iteratively re-weighted MAD transformation Remote Sens. Environ. 112 1025–36

Gutiérrez-Vélez V H and DeFries R 2013 Annual multi-resolution detection of land cover conversion to oil palm in the Peruvian Amazon Remote Sens. Environ. 129 154–67 Online: http://dx.doi.org/10.1016/j.rse.2012.10.033

Nelson B W, Mesquita R, Pereira J L G, Souza S G a, Batista G T and Couto L B 1999 Allometric Regressions for Improved of Secondary Forest Biomass in the Central Amazon For. Ecol. Manage. 117 149–67

USGS 2017. Landsat 4-7 climate data record (CDR) surface reflectance. Available at: https://landsat.usgs.gov/sites/default/files/documents/ledaps_product_guide.pdf

Zhu Z and Woodcock C E 2012 Object-based cloud and cloud shadow detection in Landsat imagery Remote Sens. Environ. 118 83–94 Online: http://dx.doi.org/10.1016/j.rse.2011.10.028

Zhu Z, Wang S and Woodcock C E 2015 Improvement and expansion of the Fmask algorithm: Cloud, cloud shadow, and snow detection for Landsats 4-7, 8, and Sentinel 2 images Remote Sens. Environ. 159 269–77 Online: http://dx.doi.org/10.1016/j.rse.2014.12.014

Table S1: Landsat images used for classification (images for 2000-2010 were classified in Gutierrez Velez and DeFries 2013).

Year	Julian date	Satellite	Path/row
1985	195	Landsat TM	06-066
1985	218	Landsat TM	07-066
1987	185	Landsat TM	06-066
1987	96	Landsat TM	07-066
1988	204	Landsat TM	06-066
1988	211	Landsat TM	07-066
1989	190	Landsat TM	06-066
1989	221	Landsat TM	07-066
1990	225	Landsat TM	06-066
1990	216	Landsat TM	07-066
1991	164	Landsat TM	06-066
1991	219	Landsat TM	07-066
1993	192	Landsat TM	07-066
1993	217	Landsat TM	06-066
1995	207	Landsat TM	06-066
1995	262	Landsat TM	07-066
1996	265	Landsat TM	07-066
1996	114	Landsat TM	06-066
1997	180	Landsat TM	06-066
1997	251	Landsat TM	07-066
1998	247	Landsat TM	06-066
1998	142	Landsat TM	07-066
1999	218	Landsat TM	06-066
1999	233	Landsat ETM+	07-066
2000	189	Landsat TM	06-066
2000	244	Landsat TM	07-066
2001	215	Landsat TM	06-066
2001	182	Landsat TM	07-066
2002	250	Landsat TM	06-066
2003	141	Landsat ETM+	06-066
2003	4	Landsat TM	07-066
2003	236	Landsat ETM+	07-066
2004	216	Landsat TM	06-066
2004	31	Landsat TM	07-066
2005	186	Landsat TM	06-066
2005	209	Landsat TM	07-066
2006	221	Landsat TM	06-066
2006	148	Landsat TM	07-066

2007	184	Landsat ETM+	06-066
2007	183	Landsat ETM+	07-066
2008	195	Landsat TM	06-066
2008	227	Landsat TM	06-066
2008	202	Landsat TM	07-066
2009	181	Landsat TM	06-066
2009	156	Landsat TM	07-066
2010	184	Landsat TM	06-066
2010	332	Landsat TM	07-066
2011	203	Landsat TM	06-066
2011	226	Landsat TM	07-066
2013	208	Landsat OLI	06-066
2013	231	Landsat OLI	07-066

Figure S1: Relationship between AGB and age in 30 field plots.

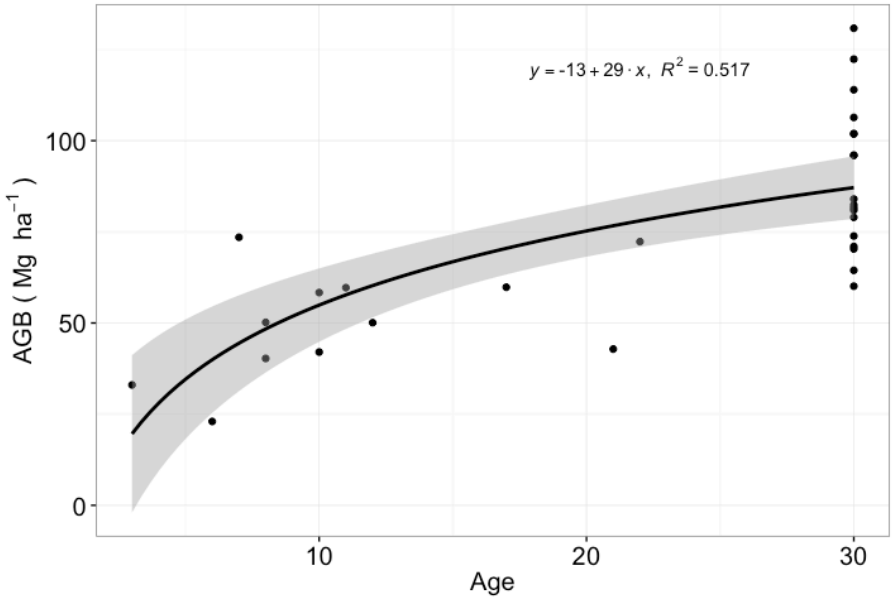

Figure S2: Plot of proportion of pixels with predicted probability of regrowth that actually re-grew. The solid 1:1 line indicates the expected value for a model that perfect predicts probability of regrowth. Our model somewhat over-predicts regrowth.

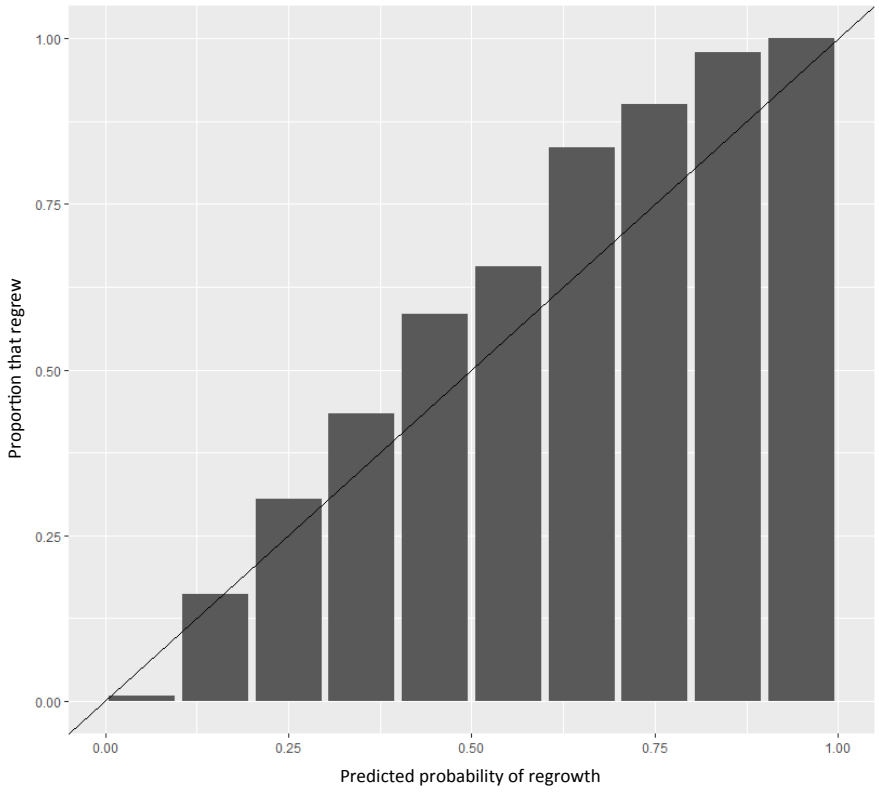
1.00
0.75
0.50
0.25
0.00
Proportion that regrew
0.00
0.25
0.50
0.75
1.00
Predicted probability of regrowth

703

Figure S3: Plot of proportion of second-growth forest pixels with predicted probability of clearing that were actually cleared. The solid 1:1 line indicates the expected value for a model that perfect predicts probability of clearing. Our model somewhat under-predicts clearing.

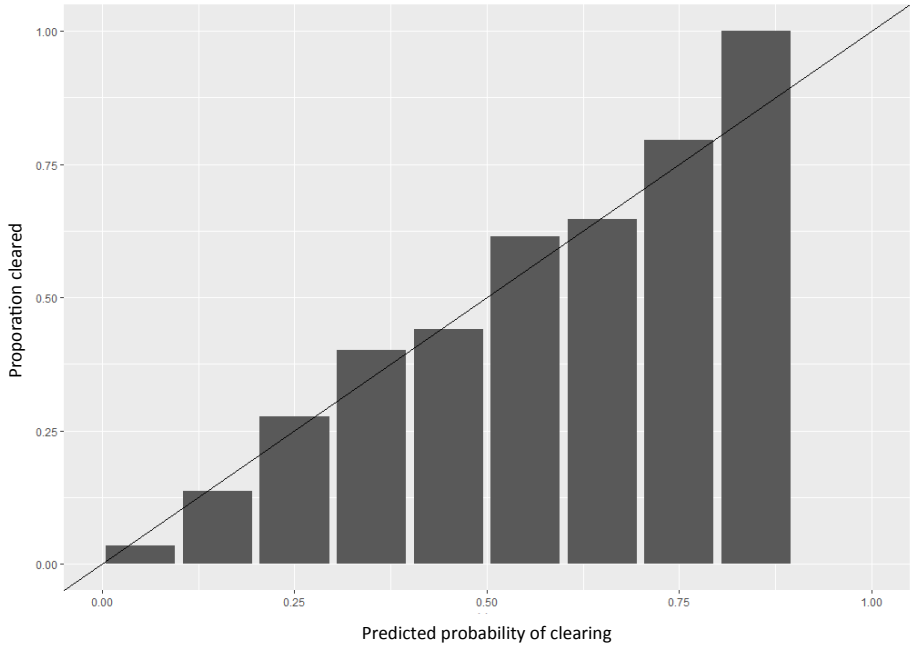

Figure S4: Distribution of forest ages in 2013.

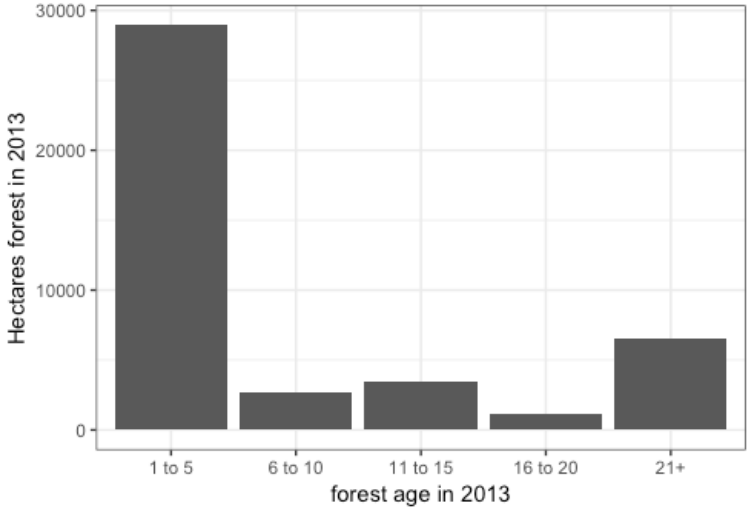

Figure S5: Inter-annual variability in probability of clearing and regrowth. Y-axis is the year-specific intercept from the mixed-effects models, i.e. the probability of event (forest regrowth, or second-growth forest clearing) at mean values for all predictors.